# Two Dimensional Modeling of a Two-Layer Porous Burner for Household Applications under the Influence of a Radiation Field

**M. M. Keshtkar***
Department of Mechanical Engineering,
Islamic Azad University, Kerman Branch, Iran
E-mail: mkeshtkar54@yahoo.com
*Corresponding author

**R. Janati Far**
Department of Mechanical Engineering,
Shahid Bahonar University, Kerman, Iran
E-mail: rjanatifar@yahoo.com

**Abstract:** This work presents a numerical study to investigate the heat transfer characteristics of a 2-D rectangular composite porous radiant burner (CPRB). In the construction of porous burner, the porous layer is considered to be composite consisting of upstream and downstream layers with equal thickness but with different physical and radiative properties. In the present work, a two dimensional rectangular model is used to solve the governing equations for porous medium and gas flow. In order to analyze the thermal characteristics of the CPRB, the coupled energy equations for the gas and porous medium are solved numerically and the discrete ordinates method is used to obtain the distribution of radiative heat flux in the porous media. Finally, the effects of the various factors on the performance of CPRB are determined. Computational results show that the high porosity and low scattering coefficient for downstream porous layer are desirable for maximizing the CPRB efficiency in comparison to homogeneous one. Comparison between the present results with those obtained by other investigators indicates a good agreement.

**Keywords:** Composite Porous Radiant Burners, Discrete Ordinates Method, 2-D Radiation Field

## 1 INTRODUCTION

Combustion in porous burners differs significantly from free flames due to two main factors including the high surface area of the porous media resulting in efficient heat transfer between the gas and the solid, and well mixing of fuel and oxidant in porous media increasing effective diffusion and heat transfer in the gas phase. In the upstream region of the combustion zone, heat is transferred from solid phase to inlet fuel-air mixture that makes preheating and in the downstream, heat of combustion is transferred from hot gas products to solid phase which in turn radiates to its surrounding [1]. This radiative converter has been applied to various industrial furnaces and has attained remarkable energy saving and combustion enhancement [2], [3]. Flames in porous media have higher burning velocities and leaner flammability limits than open flames. These effects are the consequence of phenomena named "excess enthalpy combustion" [4], where thermal energy that is generated in the combustion zone is transferred by radiation and conduction through the solid matrix to the unburned gases.

For the first time, in the field of using porous media in thermal systems, a study by Echigo [5] showed that with an appropriate choice of optical thickness of the permeable media, up to 60 percent of the non- radiating gas energy can be saved due to energy conversion from gas enthalpy to thermal radiation. The essential assumptions introduced in that study are that the system is one-dimensional and steady and scattering in the porous medium is negligible. Wang and Tien [6] extended Echigo's analysis by taking the effect of radiation scattering in the analysis. They demonstrated that the radiation scattering has important effect on the effectiveness of the energy conversion system.

Tong and Sathe [7] analyzed a PRB considering one-dimensional (1-D) solution. They used a 1-D conduction, convection and radiation model, while combustion was treated as a spatially dependent heat generation zone. For radiative part, they used spherical harmonic method. Numerical results showed that the radiative output from a porous burner depends strongly on optical properties of porous layer. Echigo et al. [8] investigated the use of porous media for combustion augmentation by considering a heat generation zone inside a porous medium. They realized that the energy recirculation by radiation preheated the combustion mixture, resulting in significant combustion augmentation.

Sathe and Tong [9] extend their earlier work by considering the actual combustion phenomena instead of constant heat generation zone. They found that for maximizing radiant output, the optical depth should be large and the flame should be stabilized near the center of porous medium.

Mital et al. [10] proposed a two section burner. The downstream layer was found to absorb heat from the hot products and redistribute it; only a small portion of the radiation was transported to the upstream section of the burner due to the small pore diameter of upstream section. The upstream section absorbed radiation at the interface of the two sections, which aided in stabilizing the flame. Fu et al. [11] investigated the thermal performance of porous radiant burners with considering an axisymmetric two-dimensional model. The results were compared with available experimental data for the purpose of model validation. Parametric calculations were performed using the model to improve understanding of the phenomena.

Leonardi et al. [12] investigated a theoretical model to predict the thermal performance of inert direct-fired, woven-metal fiber-matrix porous radiant burner. The calculated results for the burner surface temperature, the gas exhaust temperature and the radiation efficiency for a single layer burner were compared with experimental data and good agreement was obtained. Li et al. [13] developed a physical and mathematical model for simulate the directional radiative behavior of a porous radiant burner, in which the energy equations of tube wall and air are solved by finite- volume method, and the radiative source terms are determined by the Monte Carlo method. The effects of relating parameters on the directional behavior of radiative heating and the radiation heating efficiency were analyzed.

Talukdar et al. [14-15] analyzed a two-dimensional PRB with detailed radiation model. Both transient and steady state characteristics were studied. The combustion was considered as a spatially dependent heat generation zone. The energy equations for gas and solid phases were solved numerically such that the radiative part was found using the collapsed dimension method. It must be noted that, this method needs a very complicated computations for determining the radiative flux distribution in an emitting, absorbing and scattering media.

A 2-D rectangular porous burner was investigated by Mishra et al. [16]. The governing equations consist of two energy equations for gas and solid phases were solved numerically for Methane-air combustion. The radiative part of the energy equation is modeled using the collapsed dimension method. They studied the effects of equivalence ratio, extinction coefficient and volumetric heat transfer coefficient on temperature and concentration profiles.

Thermal analysis of a homogeneous porous radiant burner (PRB) was carried out by the author using the discrete ordinates method and a 2-D coordinate system [17]. In that work, a non-uniform combustion heat zone

was considered as energy source in the proposed PRB. It was found that, using porous layers with large aspect ratio and with small scattering albedo, causes an increase in the system efficiency to convert more energy from gas enthalpy to thermal radiation.

Study of literatures shows that there are a few research works about analysis of composite porous burners. In the present research, it is attempted to use more accurate model for obtaining thermal behavior of such systems. Therefore, the purpose of present work is to develop a mathematical model to investigate the thermal characteristics of a composite porous radiant burner (CPRB) using 2-D rectangular coordinate. The burner is constructed with upstream and downstream porous layers, such that the combustion zone takes place just at the middle of porous burner Fig 1.
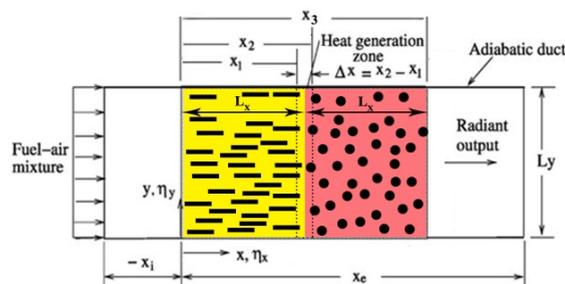


**Fig. 1**    Schematic diagram of the problem under consideration

Upstream and downstream layers have equal thickness but different properties. The model was developed to serve as a tool to support the design and optimization of different components in the CPRBs. Subsequently, numerical simulations were performed in order to clarify the complex heat transfer mechanisms and to gain some guidance for the design of the CPRBs.

The analysis here employs discrete ordinates method for computing radiative heat flux in the burner, whereas, this method remains simple in expressions but retains important physical insights. As a result of high porosity of porous medium, thermal conductivity in this medium is low, and thus it is assumed that only convection and radiation take place in the porous matrix.

However, in the gas flow, because of non–radiative gas assumption, heat transfer occurs by conduction and convection. In the present analysis, an attempt is made to investigate the effects of radiation properties of the upstream and downstream layers on the performance of the CPRB. Besides, the thermal behavior of CPRB is compared to conventional homogeneous one. For validation, the numerical results are compared with theoretical and experimental results of other investigators and good agreement is found.

## 2    THEORETICAL ANALYSIS

The problem under consideration is schematically shown in Fig. 1. The CPRB consists of two porous layers attached to each other which are indicated by zone 1 and 2, respectively. The composite porous matrix is assumed to be gray and isotropically emitting, absorbing and scattering media and its thickness in the flow direction is $2L_x$=20 mm. Combustion zone, representing the flame, is situated in the region $x_1 < x < x_2$. The porous burner is located between two parallel adiabatic and refractory plates which are the duct's walls.

A gaseous fuel–air mixture enters the duct at $x = -x_i$. The fluid velocity $u_g$ is constant everywhere and the temperature distribution $T_g$ is assumed uniform over every cross-section. The slug flow is assumed to be steady and laminar. Gaseous radiation is neglected in comparison to solid radiation, thus radiation is considered only between the particles that comprise the porous layer. All thermo physical properties of the solid and the gas phases for each layer are assumed constant.

Since the solid and gas phases are not in local-thermal equilibrium, separate energy equations are needed to describe energy transfer in these two phases. The governing equations inside the porous region which are the energy equations for the fluid flow and porous segment may be written as follows:

$$\nabla.(\varphi \rho_g u_g c_p T_g) = \nabla.(\varphi k_g \nabla T_g) - (1-\varphi)hA(T_g - T_p) \atop + \varphi \dot{Q}(y)\delta(x) \tag{1}$$

$$0 = (1-\varphi)hA(T_p - T_g) \atop - \nabla.((1-\varphi)k_p \nabla T_p) - \nabla.q_r \tag{2}$$

In the above equations, A is the surface area per unit volume of the solid phase and h is the heat transfer coefficient between the fluid and the solid matrix. The subscripts "g" and "p" stand for gas and solid phases respectively. In solving the energy equation, it should be considered that the thermo-physical properties of porous media in upstream and downstream layers such as optical thickness, conductivity and scattering coefficient are different. The term $\delta(x)$ is the delta function defined as unity for $x_1 \le x \le x_2$ and zero elsewhere and $\dot{Q}(y)$ is the non-uniform heat generation with a parabolic polynomial, therefore maximum heat released takes place at the mid-plan and the minimum values near the solid walls.

In the region sufficiently far from the porous layer so that the temperature gradient is low, the conduction term in the energy equation for the gas flow is

neglected. For parametric studies, the governing equations and the boundary conditions are non–dimensionalized by introducing the dimensionless parameters which are given in Table 1.

**Table 1**  Non–dimensional parameters of the test case from Tong and Sathe [7]

| Parameter | Value |
|---|---|
| $\lambda_1 = \rho_g u_g c_g T_i / \dot{Q} L_x$ | 0.014 |
| $\lambda_2 = hAT_i / \dot{Q}$ | 4 |
| $\lambda_3 = k_g T_i / \dot{Q} L_x^2$ | 0.00025 |
| $\lambda_4 = k_p T_i / \dot{Q} L_x^2$ | 0.02 |
| $\lambda_5 = hL_x / k_p$ | 5 |
| $\lambda_6 = \varepsilon k_p / \sigma T_i^3 L_x$ | 0 |

Using these dimensionless groups, the non–dimensional forms of the governing equations in the region $0 \le x \le x_3$ can be obtained as follows:

$$\varphi \lambda_1 \frac{\partial \theta_g}{\partial \eta_x} = -(1-\varphi)\lambda_2 (\theta_g - \theta_p)$$
$$+ \varphi \lambda_3 (\frac{\partial^2 \theta_g}{\partial \eta_x^2} + \frac{\partial^2 \theta_g}{\partial \eta_x^2}) + \varphi \delta(x) \tag{3}$$

$$0 = (1-\varphi)\lambda_2 (\theta_p - \theta_g)$$
$$- (1-\varphi)\lambda_4 (\frac{\partial^2 \theta_p}{\partial \eta_x^2} + \frac{\partial^2 \theta_p}{\partial \eta_y^2}) - \nabla Q \tag{4}$$

Equations (3) and (4) are to be solved by prescribing appropriate boundary conditions. At the inlet $(x = -x_i)$, the gas is at the ambient temperature $T_i$, and at the outlet $(x = x_e)$, adiabatic condition is assumed to prevail and the top and bottom walls of the duct are considered to be adiabatic. For the solid phase, at axial sections $\eta_x = 0$ and 1, the mechanism of heat transfer between solid and gas is by convection and radiation. Eqs. (3) and (4) are solved simultaneously with the boundary conditions presented above. The readers are referred to the reference [17] for more details.

To determine the radiative heat flux, the solid and gas phases are considered as a single homogeneous phase and the radiative transfer equation is solved. The heat source/sink term, $\nabla \cdot q$ due to radiation in solid phase that appears in Eq. (4), is calculated from Eq. (5):

$$\nabla q = \sigma_a(r) \left( 4\pi I_b - \int_{4\pi} I(r,s)d\Omega \right) \tag{5}$$

Radiative intensity is obtained by solving the radiative transfer equation:

$$\frac{dI(\vec{r},\hat{s})}{ds} = \hat{s}.\nabla I(\vec{r},\hat{s}) =$$
$$-(\sigma_a(\vec{r}) - \sigma_s(\vec{r}))I(r,\hat{s}) + S(\vec{r},\hat{s}) \tag{6}$$

where the source function is:

$$S(\vec{r},\hat{s}) = \sigma_a(\vec{r})I_b(\vec{r})$$
$$+ \frac{\sigma_s(\vec{r})}{4\pi} \int_{4\pi} I(\vec{r},\hat{s}')\varphi(\hat{s}',\hat{s})d\Omega' \tag{7}$$

where $\sigma_s$ is the scattering coefficient and $\phi(\hat{s}',\hat{s})$ is the scattering phase function. The radiation intensity $I(\vec{r},\hat{s})$ is a function of position and direction. The expression on the left-hand side represents the gradient of the intensity in the specified direction $\hat{s}$.

According to DOM, equation (6) is solved for a set of n different directions $s_i=1,2,\ldots,n$ and the integrals over direction are replaced by numerical quadratures. Therefore, the radiative transfer equation is approximated by a set of n differential equations, as follows [18]:

$$\frac{dI(\vec{r},\hat{s}_i)}{ds} = \hat{s}.\nabla I(\vec{r},\hat{s}_i) = \sigma_a(\vec{r})I_b(\vec{r}) - \beta(\vec{r})I(\vec{r},\hat{s}_i)$$
$$+ \frac{\sigma_s(\vec{r})}{4\pi} \sum_{j=1}^{n} w_j I(\vec{r},\hat{s}'_j)\varphi(\vec{r},\hat{s}_i,\hat{s}_j) \qquad i=1,2,\ldots,n \tag{8}$$

Where the $w_j$ are the quadrature weights associated with the directions $s_i$. This equation is subjected to the following boundary condition on the surface boundaries:

$$I(r_w,\hat{s}) = \varepsilon(r_w)I_b(r_w) + \frac{\rho(r_w)}{\pi} \sum_{\hat{n}\hat{s}_j<0} I(r_w,\hat{s}_j)|\hat{n}\hat{s}_j|w_j \tag{9}$$
$$\text{for:} \qquad \hat{n}\hat{s}_i > 0$$

For the two-dimensional Cartesian geometry, the RTE can be expressed for each individual ordinate direction $m$, as follows [19]:

$$\mu^m \frac{\partial I^m}{\partial \eta_x} + \zeta^m \frac{\partial I^m}{\partial \eta_y} = \sigma_a I_b - \beta I^m + \frac{\sigma_s}{4\pi} \sum_{m'} w^{m'} I^{m'} \tag{10}$$

Where $m$ and $m'$ denote outgoing and incoming directions, while $\mu^m$ and $\xi^m$ are the direction cosines of a discrete direction. In this way Eq. (5) is written as follows:

$$\nabla q = \sigma_a(r) \left( 4\pi I_b - 4\pi \sum_{m=1}^{M} I^m \right) \tag{11}$$

Where M is the total number of ordinate directions and is related to the order of approximation $N$, though relationship $M = N(N+2)/2$.

## 3 METHOD OF SOLUTION

Non-dimensional forms of the governing equations ,(Eqs. (3), (4) and (8)) are solved numerically to obtain the temperature and radiative heat flux distributions at each nodal point in the 2-D computational domain along the burner. Equations (3), (4) and (8) are coupled and must be solved simultaneously. For this purpose, the finite-difference forms of the gas and porous energy equations are obtained using the central differencing for derivative terms.

The governing equations are discretized in a uniform structural mesh, where the error of discretization is the order of $(\Delta x)^2$ and $(\Delta y)^2$. Grid independency is checked for some mesh points and finally a uniform mesh $40 \times 100$ is selected in x and y-directions. The discrete ordinates method is used to transform the equation of radiative transfer to a set of ordinary differential equations, which are numerically solved simultaneously with the gas and solid energy equations. The sequence of calculations can be stated as follows:

1- A first approximation for the temperature and the radiative heat flux distribution is assumed.
2- Radiative transfer equation is solved for obtaining the value of intensity, radiative heat flux distribution and divergence of radiative heat flux at each nodal point using S6 approximation.
3- Using the radiative heat flux distribution which is obtained in step 2, the solid energy equation is solved to calculate porous temperature $\theta_p$.
4- The finite difference form of gas energy equation is solved for obtaining the value of $\theta_g$ at each nodal point.
5- Steps 2 to 4 are repeated until convergence is achieved.

Convergence for step 5 was assumed to have been achieved when the fractional changes in the temperature and radiative flux between two consecutive iteration levels did not exceed $10^{-4}$ at each grid point. For this purpose, 500 to 900 iterations for overall simulation were required, depending on the operating condition.

## 4 VALIDATION OF COMPUTATIONAL RESULTS

To validate the computational results, a homogeneous porous radiant burner as a test case was analyzed and the results were compared with the theoretical data given in reference [7]. The values of non-dimensional

parameters for this test case which are the same as used by Tong and Sathe [7] are given in "Table 1". It is seen that the maximum gas temperature occurs inside the heat generation zone such that radiation serves as a mechanism for heat removal from this region [17].

The technique of energy conversion between gas enthalpy and thermal radiation by means of porous medium has been used in energy saving systems to recover as much as possible of the residual energy from exhaust or wasted gas flow in high temperature systems. Therefore, in order to confirm the validity of the present analysis for the energy conversion between gas enthalpy and thermal radiation, a test case is analyzed and the numerical computations are compared with the theoretical results given in references [5] and [6]. The values of non-dimensional parameters for this test are given in Table 2.

**Table 2** Non–dimensional parameters of the test case

| parameter | Value |
|-----------|--------|
| $\lambda_1$ | 0.015 |
| $\lambda_2$ | 0.75 |
| $\lambda_3$ | 0.0003 |
| $\lambda_4$ | 0.03 |
| $\lambda_5$ | 3.5 |
| $\lambda_6$ | 54.3 |
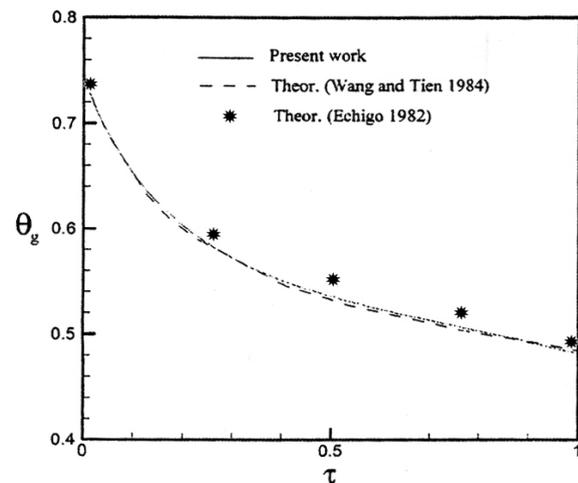


**Fig. 2** Gas temperature distribution inside the porous layer

The variation of gas temperature inside the porous layer for the test case is shown in Fig. 2 in order to make a comparison between the results of the present computations and the theoretical predictions of other investigators. There is a considerable temperature drop in the gas flow, especially at the entrance of the layer. This is a marker for the basic principle of energy conversion. However, Fig. 2 shows a good consistency between the present results and those obtained in these references.
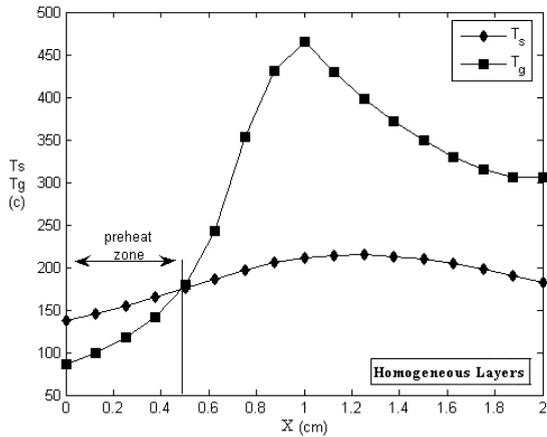
(a): Gas and porous temperature distributions
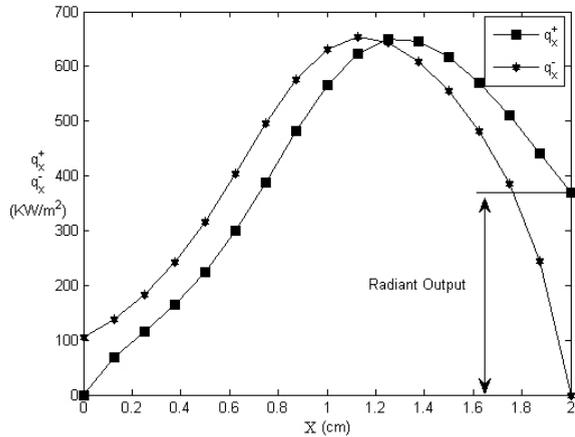


(b): Radiative heat flux distributions at the mid-plan, y=$L_y$/2

**Fig. 3**    Temperature and radiative heat flux distributions in the PRB with homogeneous layers $\varphi_1 = \varphi_2 = 0.93$,

$$\beta_1 = \beta_2 = 100, \omega_1 = \omega_2 = 0.5$$

## 5    RESULTS AND DISCUSSION

In order to show the thermal behavior of the CPRB, the gas and porous temperature profiles $\theta_g, \theta_p$ and also the variation of radiative fluxes $q_x^+, q_x^-$ along a homogeneous burner at the mid-line (y=$L_y$/2) are shown in Fig. 3. It should be mentioned that for analyzing a homogeneous burner, the upstream and downstream layers which are attached to each other are the same.

The heat generation zone position represented by $\zeta_{fl} = (x_1 + x_2)/2x_3$ is equal to 0.5, that is, the flame was regarded as suited in the middle of porous segment. It should be noted that in the computation of Fig. 3, the thickness of combustion zone, i.e. $x_2 - x_1$ is considered equal to 0.2cm.

Fig. 3(a) shows that the gas and porous temperatures increase along the flow direction at the entrance of the burner, such that maximum values of these variables occur in the combustion zone. For the radiative heat fluxes, Fig. 3(b) shows that the maximum value of $q_x^+$ and $q_x^-$ occur outside the combustion zone. The value of downstream radiative flux $q_x^+$ at $x = x_3$ is the radiative output which is very important in improving the radiant burner efficiency.
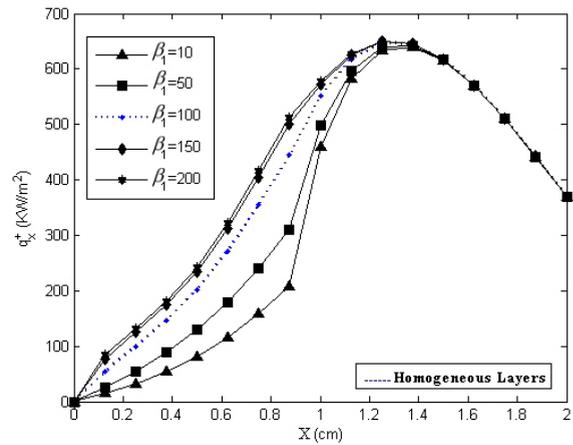


(a): Effect of absorption coefficient of the upstream layer on radiative heat flux
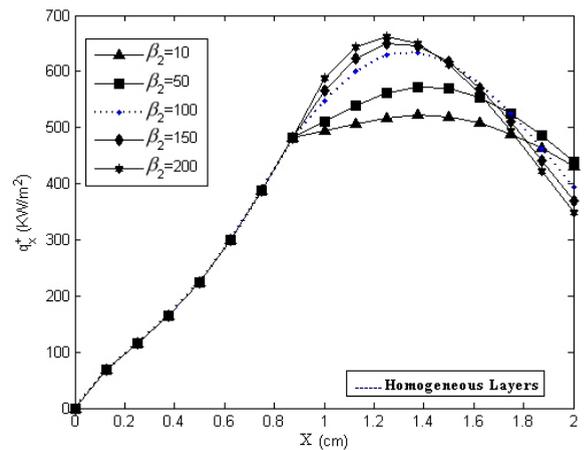


(b): Effect of absorption coefficient of the downstream layer on radiative heat flux

**Fig. 4**    Effect of the absorption coefficient on the radiative flux distributions at centerline $\varphi_1 = \varphi_2 = 0.93$, $\omega_1 = \omega_2 = 0.5$

In the computation of Fig. 3, the thickness of each layer in porous burner $L_x$, is equated to 1 cm. For a composite porous burner, Fig. 4(a) shows the effect of the absorption coefficient on the radiative heat flux distribution with different extinction coefficients for

upstream layer, while the extinction coefficient for downstream layer is kept constant.

It is seen that the extinction coefficient of the upstream layer does not have a considerable effect on the burner radiant output. But, if one notices to Fig. 4(b), it can be concluded that the extinction coefficient of the downstream layer has a main role on generating the radiant output, such that as the value of $\beta_2$ increases in a certain range, the radiant output of CPRB increases by converting more of the convective energy to radiative energy, but higher value of $\beta_2$ results in a lower radiant output from the CPRB. The optimal value of $\beta_2$ depends on radiative properties of porous layers.

Also for comparison, operation of porous burner with homogeneous layer is shown at this figure.

One of important factors in the performance of CPRBs is the porosity of layers. The effect of porosity for upstream layer on radiative heat flux, $q_x^+$ along the flow direction is shown in Fig. 5(a). It is seen that for all cases, the maximum values of radiant output remains almost constant and variation of upstream layer porosity is not effective on the performance of CPRB. But in Fig. 5(b) it is seen that, the radiant output at the outlet section increases as the porosity value of downstream layer $\phi_2$ increases, such that the porosity about 0.93 seems enough to obtain the sufficient efficiency and the higher values of $\phi_2$, decreases the value of radiant output. It is due to this fact that the porosity has two folds effects on the radiative out put such that, by increasing the porosity from a small value, the amount of surface area for convection process between gas flow and solid phase increases that leads to increase the burner radiant output. But further increase in the porosity, causes a decrease in the number of solid particles in unit volume of the porous layer and therefore, decrease in the radiative heat flux from the solid phase.
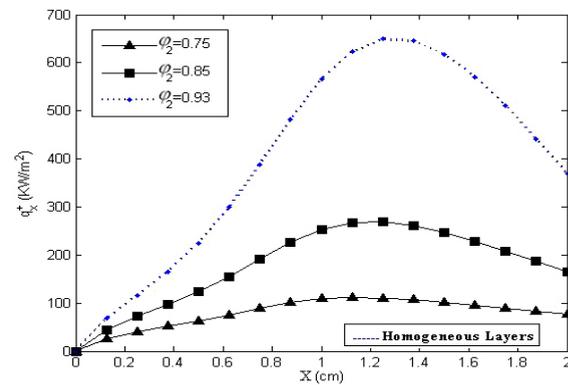


(b): Variation of the porosity for downstream layer

**Fig. 5**    Effect of the porosity on the radiative flux distributions at mid-line $\beta_1 = \beta_2 = 100,\ \omega_1 = \omega_2 = 0.5$
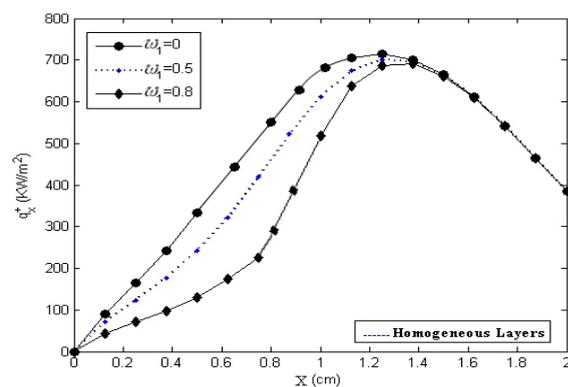


(a): Variation of the scattering albedo for upstream layer
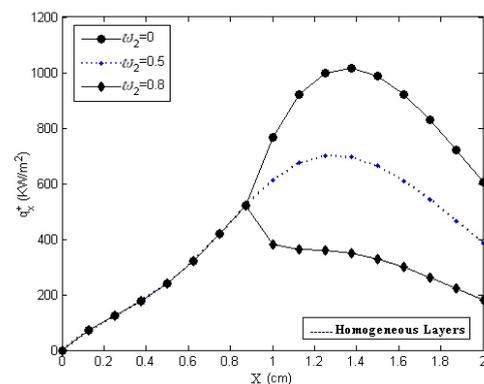


(b): Variation of the scattering albedo for downstream layer

**Fig. 6**    Effect of the scattering albedo on the radiative flux distributions $\beta_1 = \beta_2 = 100,\ \varphi_1 = \varphi_2 = 0.93$

The effect of scattering albedo on radiative heat flux distribution, $q_x^+$ along the flow direction is shown in Fig. 6. The variations of radiant output for three different values of scattering albedo for upstream layer is shown in Fig. 6(a). This figure shows that there is not



(a): Variation of the porosity for upstream layer

a considerable variation of radiative output at different scattering albedo. Besides, It is seen in Fig. 6(b) that a lower scattering albedo for downstream results in a higher radiative heat flux along the burner and also higher radiant output.

## 6    CONCLUDING REMARKS

A two-dimensional numerical study of heat transfer within composite porous radiant burner has been conducted. The system has two porous layers, which have equal thickness and different radiative properties. In the combustion zone, a non-uniform generation is used to simulate combustion process and radiation of the solid phase is taken into consideration using S6 discrete ordinate approximation for calculation of radiative heat fluxes but the gas phase is considered to be non-radiating media.

Computational results show that the material and structure of downstream layer have significant influences on the radiant output and efficiency in the CPRB. The results show that a composite porous burner with an optimal absorption coefficient and small scattering albedo for downstream layer causes a large radiant output at the outlet of the CPRB. Also, it is found that, the downstream layer with high porosity, operates efficiently. Finally, the three parameters $\beta_2, \varphi_2$ and $\omega_2$ for the downstream layer are found to be the main design parameters for this type of CPRB.

## 7    NOMENCLATURE

| | |
|---|---|
| $B$ | Incoming radiation (W/m$^2$) |
| $B'$ | Non-dimensional incoming radiation, $B / \dot{Q} L_x$ |
| $L_x$ | Length of porous layer (m) |
| $L_y$ | Height of porous layer (m) |
| $\beta$ | Extinction coefficient (m-1) |
| $\varepsilon$ | Emissivity |
| $\sigma$ | Stefan-boltzmann constant (W/m2K4) |
| $\sigma_a$ | Absorption coefficient (m-1) |
| $\sigma_s$ | Scattering coefficient (m-1) |
| $\varphi$ | Porosity |
| $\omega$ | Scattering albedo, $\sigma_s / \sigma_e$ |

## REFERENCES

[1]    Bengue, J. P. and Saveliev, A. V., "Super adiabatic combustion of methane air mixtures under filtration in packed bed", Combustion and Flame, Vol. 100, 1998, pp. 221-231.

[2]    Hoffman, J. G. and Echigo, R., "An experimental study on combustion in porous media with a reciprocating flow system", Combustion and Flame, Vol. 111, 1997, pp. 32-46.

[3]    Zhdanok, S. and Kennedy, L. A, "Super adiabatic combustion of methane air mixtures under filtration in packed bed", Combustion and Flame, Vol. 100, 1995, pp. 221-231.

[4]    Takeno, T. and Sato, K., "An excess enthalpy flame theory", Combust. Sci. Technol, Vol. 20, 1979, pp. 73-84.

[5]    Echigo, R., "Effective energy conversion method between gas enthalpy and thermal radiation and application to industrial furnaces", Proc. 7th Int. Heat Transfer Conf., München, Vol. 6, 1982, pp. 361-366.

[6]    Wang, K. Y. and Tien, C. L., "Thermal insulation in flow systems: combined radiation and convection through a porous segment", Heat Transfer, Vol. 106, 1984, pp. 453-459.

[7]    Tong, T. and Sathe, S., "Heat transfer characteristics of porous radiant burners", Trans.  of ASME, Heat Transfer, Vol. 113, 1991, pp. 423-428.

[8]    Echigo, R., Yoshizawa, Y., Hanamura, K. and Tomimura, T., "Analytical and experimental studies on radiative propagation in porous media with internal heat generation", Proc., 8th Int. Heat Transfer Conf., 1986, pp. 827-832.

[9]    Sathe, S. B. and Tong, T. W., "A numerical analysis of heat transfer and combustion in porous radiant burners", Int. J. Heat and Mass Transfer, Vol. 33, 1990, pp. 1331-1338.

[10]   Mital, R., Gore J. P., Viskanta, R., and Mcintosh A. C., "An experimental evaluation of asymptotic analysis of radiant burners", Symposium on Combustion, Vol. 27, 1998, pp. 3163-3171.

[11]   Fu, X., Viskanta, R., and Gore, J. P., "Combustion and heat transfer interaction in a pore-scale refractory tube burner", Thermophysics and Heat Transfer, Vol. 12, 1998, pp. 164-171.

[12]   Leonardi, S. A., Viskanta, R., and Gore J. P., "Analytical and experimental study of combustion and heat transfer in submerged flame metal fiber burners/heaters", Heat Transfer, Vol. 125, 2003, pp. 118-125.

[13]   Li, B. X., Lu, Y. P., and Liu, L. H., "Analysis of directional radiative behavior and heating efficiency for a gas- fired radiant burner", Quantitative Spectroscopy & Radiative Transfer, Vol. 92, 2005, pp. 51-59.

[14]   Talukdar, P., Mishra, S., Trimis, D. and Durst, F., "Heat transfer characteristics of a porous radiant burner under the influence of a 2–D radiation field", Quantitative Spectroscopy & Radiative Transfer, Vol. 1-11, 2003.

[15]   Talukdar, P. and Mishra, S. C., "Analysis of conduction–radiation problem in absorbing–emitting and anisotropically scattering media using the collapsed dimension method", Heat Mass Transfer, Vol. 45, 2002, pp. 2159-2168.

[16]   Mishra, S. C., Steven, M. Nemoda, S., Talkudar, P., Trimis, D. and Durst, F., "Heat transfer analysis of a

two dimensional rectangular porous radiant burner", Heat and Mass Transfer, Vol. 33, 2006, pp. 467-474.

[17]    Keshtkar, M. M. and Gandgalikhan Nassab, S. A., "Theoretical analysis of porous radiant burners under 2-D radiation field using discrete ordinates method", Quantitative Spectroscopy & Radiative Transfer, Vol. 32, 2009, pp. 117-125.

[18]    Fiveland, W. A., "Discrete- ordinates solution of the radiative transport equation", Heat Transfer, Vol. 106, 1984, pp. 699 - 706.

[19]    Modest, M. F., Radiative Heat Transfer, New York: McGraw-Hill book Company, 1993.